

Transcriptomic Analyses of Xylan Degradation by *Prevotella bryantii* and Insights into Energy Acquisition by Xylanolytic Bacteroidetes^{*[5]}

Received for publication, May 5, 2010, and in revised form, June 11, 2010. Published, JBC Papers in Press, July 9, 2010, DOI 10.1074/jbc.M110.141788

Dylan Dodd^{†‡§¶}, Young-Hwan Moon^{§¶}, Kankshita Swaminathan^{§¶||}, Roderick I. Mackie^{§¶||**}, and Isaac K. O. Cann^{†§¶||**1}

From the [†]Department of Microbiology, [§]Energy Biosciences Institute, [¶]Institute for Genomic Biology, and Departments of ^{||}Crop Sciences and ^{**}Animal Sciences, University of Illinois, Urbana, Illinois 61801

Enzymatic depolymerization of lignocellulose by microbes in the bovine rumen and the human colon is critical to gut health and function within the host. *Prevotella bryantii* B₁₄ is a rumen bacterium that efficiently degrades soluble xylan. To identify the genes harnessed by this bacterium to degrade xylan, the transcriptomes of *P. bryantii* cultured on either wheat arabinoxylan or a mixture of its monosaccharide components were compared by DNA microarray and RNA sequencing approaches. The most highly induced genes formed a cluster that contained putative outer membrane proteins analogous to the starch utilization system identified in the prominent human gut symbiont *Bacteroides thetaiotaomicron*. The arrangement of genes in the cluster was highly conserved in other xylanolytic Bacteroidetes, suggesting that the mechanism employed by xylan utilizers in this phylum is conserved. A number of genes encoding proteins with unassigned function were also induced on wheat arabinoxylan. Among these proteins, a hypothetical protein with low similarity to glycoside hydrolases was shown to possess endoxylanase activity and subsequently assigned to glycoside hydrolase family 5. The enzyme was designated PbXyn5A. Two of the most similar proteins to PbXyn5A were hypothetical proteins from human colonic *Bacteroides* spp., and when expressed each protein exhibited endoxylanase activity. By using site-directed mutagenesis, we identified two amino acid residues that likely serve as the catalytic acid/base and nucleophile as in other GH5 proteins. This study therefore provides insights into capture of energy by xylanolytic Bacteroidetes and the application of their enzymes as a resource in the biofuel industry.

The hydrolysis and fermentation of plant cell wall polysaccharides are important metabolic processes that occur within the gut ecosystem of ruminants as well as humans. Xylan is the most abundant plant polysaccharide after cellulose, and microbes within the bovine rumen have evolved to efficiently degrade this hemicellulosic substrate. The depolymerization of

xylan requires the coordinated action of a number of enzymes, including endoxylanases, β -xylosidases, α -L-arabinofuranosidases, α -glucuronidases, acetylxylan esterases, and ferulic acid esterases (1). *Prevotella* spp. are the most numerically dominant xylanolytic bacteria in the rumen (2, 3); therefore, the mechanism by which they degrade and utilize xylan has been an important topic of investigation (4–9). *Prevotella bryantii* B₁₄ is frequently isolated from the rumen microbiome and can grow with xylan as the sole carbohydrate source (6). However, to date only six genes with roles in xylan hydrolysis have been cloned and characterized from *P. bryantii* B₁₄, including two glycoside hydrolase (GH)² family 10 endoxylanases (7, 8, 10), three GH family 3 β -xylosidases (4), and one GH family 43 β -xylosidase enzyme (7, 8). Given the capacity of this organism to grow efficiently with xylan substrates and considering the complexity in chemical linkages within natural xyans, it is likely that *P. bryantii* B₁₄ uses additional as yet unidentified enzymes to degrade xylan.

The genome of *P. bryantii* B₁₄ has recently been partially sequenced (11), and this bacterium harbors at least 109 genes predicted to encode either glycoside hydrolases or carbohydrate esterases. In this study, a transcriptional approach was employed to identify the genes harnessed by *P. bryantii* B₁₄ to degrade xylan. Because it has been reported that endoxylanase activity of *P. bryantii* B₁₄ is induced by medium to large sized xylo-oligosaccharides and not by monosaccharides (12), the transcriptional profile of *P. bryantii* B₁₄ cultured either with soluble wheat arabinoxylan (WAX) or with a mixture of xylose and arabinose (XA) was investigated. The studies allowed us to assemble the enzymes that likely constitute the xylan-degrading machinery of *P. bryantii* B₁₄. In addition, we have assigned biochemical function to two hypothetical proteins that were up-regulated in cells metabolizing wheat arabinoxylan compared with a mixture of its monosaccharide components. Genes encoding similar polypeptides, which invariably exhibited endoxylanase activity, were identified in several members of the Bacteroidetes, suggesting that this group of enzymes is critical to the capture of energy from xylan in this phylum. More importantly, our analyses have led to the discovery of a gene cluster, composed of an invariant core of six genes flanked by either biochemically charac-

* This work was supported by the Energy Biosciences Institute. D. D. was partially supported by National Institutes of Health Fellowship 1F30DK084726 from NIDDK.

[5] The on-line version of this article (available at <http://www.jbc.org>) contains supplemental Figs. S1–S8 and Tables S1 and S2.

¹ To whom correspondence should be addressed: 1105 Institute for Genomic Biology, 1206 West Gregory Dr., University of Illinois at Urbana-Champaign, Urbana, IL 61801. Tel.: 217-333-2090; Fax: 217-333-8286; E-mail: icann@illinois.edu.

² The abbreviations used are: GH, glycoside hydrolase; WAX, wheat arabinoxylan; HPAEC, high performance anion exchange chromatography; XA, xylose and arabinose.

Xylan Degradation in the Bacteroidetes

terized or putative glycoside hydrolases and carbohydrate esterases in *P. bryantii* B₁₄. The genes within the cluster and their collective response during wheat arabinoxylan utilization suggest that the cluster is critical to xylan utilization in this bacterium. Furthermore, the conservation of the gene cluster in other xylanolytic *Prevotella* and *Bacteroides* spp. derived from the bovine rumen and the human colonic microbiomes suggests a conserved mechanism for xylan utilization by xylanolytic Bacteroidetes.

EXPERIMENTAL PROCEDURES

Materials—*P. bryantii* B₁₄ (DSM 11371) was initially isolated by Bryant *et al.* (13) and was obtained from our culture collection in the Department of Animal Sciences at the University of Illinois, Urbana-Champaign. *Bacteroides intestinalis* 341 (DSM 17393) was a kind gift from Jeffrey I. Gordon (Washington University, St. Louis) and was originally obtained from the DSMZ (German Collection of Microorganisms and Cell Cultures, Braunschweig, Germany). *Escherichia coli* JM109 and *E. coli* BL21-CodonPlus™ (DE3) RIL competent cells and the PicoMaxx high fidelity DNA polymerase were acquired from Stratagene (La Jolla, CA). The pET-46 Ek/LIC vector kit was obtained from Novagen (San Diego). The RNeasy Protect Bacteria reagent, RNeasy mini kit, RNeasy-free DNase set, DNasey blood and tissue DNA purification kit, and QIAprep spin miniprep kit were all obtained from Qiagen (Valencia, CA). Xylo-oligosaccharides and wheat arabinoxylan (medium viscosity, 20 centistokes) were obtained from Megazyme (Bray, Ireland). The Superscript double-stranded cDNA synthesis kit and the RiboMinus transcriptome isolation kit were obtained from Invitrogen. The One-Color DNA labeling kit, hybridization kit, Sample Tracking control kit, and Wash Buffer kit were all obtained from Roche NimbleGen (Madison, WI). All other reagents were of the highest possible purity and were purchased from Sigma.

Growth of *P. bryantii* B₁₄ and Isolation of RNA—*P. bryantii* B₁₄ was grown anaerobically in a modified chemically defined medium (4) with either wheat arabinoxylan (0.15% w/v) or a mixture containing both xylose (0.0885% w/v) and arabinose (0.0615% w/v) as the sole carbohydrate sources. The concentrations of XA in the mixture were equivalent to that in the WAX polysaccharide (59:41, xylose/arabinose). Cells were subcultured two times consecutively in triplicate with the respective growth media to ensure complete adaptation to the carbohydrate growth source. At mid-log phase of growth ($A_{600\text{ nm}} = 0.2$), 30 ml of each culture was removed and immediately combined with 60 ml of RNeasy Protect Bacteria reagent, and RNA was purified using the RNeasy kit with the optional on-column DNase treatment step. The quality of the RNA was assessed by using a Bioanalyzer 2100 with a RNA 6000 Nano Assay reagent kit from Agilent (Santa Clara, CA).

Gene Expression Analysis Using DNA Microarrays—DNA microarray slides were fabricated by Roche NimbleGen (Madison, WI) using the partial genome sequence of *P. bryantii* B₁₄. Four arrays were printed on each slide, with each array containing 68,877 total probes. For each array, a total of 2551 open reading frames (ORFs) were analyzed each with nine individual probes and with three replicates per probe. The estimated

genome size for *P. bryantii* B₁₄ is 3.6 megabases, and the total number of identified features (RNAs and ORFs) is 2710. Thus, the microarrays covered ~94% of the genome features for *P. bryantii* B₁₄. The purified RNA was converted to double-stranded cDNA by using the Superscript cDNA synthesis kit. The cDNA was then labeled with Cy3 by using the One-Color DNA labeling kit, which employs Cy3-labeled random nonamer primers. Sample tracking controls were added to each of the labeled cDNA samples, and hybridization was performed at 42 °C using the hybridization kit and a MAUI® 4-bay hybridization system from BioMicro Systems (Salt Lake City, UT). After 18 h, the slides were removed, washed using the Wash Buffer kit, and scanned using a GenePix 4000B microarray scanner with the laser tuned to a wavelength of 532 nm and a photomultiplier tube gain of 680. The files were then analyzed using the NimbleScan version 2.5 software. The gene expression values were determined using ArrayStar version 3.0 from DNASTAR, Inc. (Madison, WI).

Whole Transcriptome Analysis by RNA Sequencing—For RNA-Seq analyses, the RNAs isolated from two individual experiments were used for each growth condition. Bacterial 16S and 23S ribosomal RNAs were subtracted from ~10 µg of total RNA with the RiboMinus™ bacteria transcriptome isolation kit. The enriched mRNA fraction was converted to an RNA-Seq library using the mRNA-Seq kit from Illumina Inc. (San Diego) with multiplexing adaptors that tag each library with a unique identifier. Fragments 200–400 bp long were size-selected for the final library. Each library was hybridized onto a single lane of an eight-lane flow cell and sequenced with a Genome Analyzer IIX according to the manufacturer's instructions (Illumina, Inc.). The sequences derived from each library were 73 bp long, and the overall error rate of the control lane was 0.83%. Each library yielded the following number of reads: WAX1, 11.2 million reads; WAX2, 7.1 million reads; XA1, 8.8 million reads; and XA2, 6.8 million reads.

The RNA-Seq data were analyzed using CLC genomics workbench version 3.7 from CLC Bio (Cambridge, MA). The partial genome sequence for *P. bryantii* B₁₄ was uploaded onto the Rapid Annotation using Subsystem Technology (RAST) server (14), and the annotated genome was exported as a GenBank file (.gbk). The *P. bryantii* B₁₄ GenBank file was then uploaded onto the CLC software and used as a reference genome for RNA-Seq analyses for each of the four samples. Reads were only assembled if the fraction of the read that aligned with the reference genome was greater than 0.9 and if the read matched other regions of the reference genome at less than 10 nucleotide positions. The RNA-Seq output files were then analyzed for statistical significance by using the proportion-based test of Baggerly *et al.* (15).

De Novo Assembly of the *P. bryantii* B₁₄ Transcriptome—To analyze the entire transcriptome of *P. bryantii* B₁₄, a *de novo* assembly of the RNA-Seq data was performed with 82 million 60-bp single end, nucleotide reads from a total of seven illumina lanes. These data included the four illumina libraries previously mentioned and included three additional illumina libraries. These three additional libraries were constructed with a mixture of RNA from WAX- and XA-grown cultures, in which the multiplexing adaptor reaction had failed, and the individual

RNA populations could not be separated based upon the cognate growth substrate. Thus, these libraries were not useful for analyzing differential gene expression, but they did contain information on transcript coverage and were included in the transcriptome assembly. The reads were filtered for adaptor sequences and assembled into contiguous sequences (contigs) using ABySS version 1.0.12 with *k*-mer lengths of 25, 30, 35, 40, 45, and 50. Twenty five 2.83-GHz cores, on a cluster with 200 processors with 16 gigabytes per 8 cores, were used for each *k*-mer assembly. The six different *k*-mer assemblies were merged, and any contig that shared 100% identity to a larger contig and was completely contained within the larger contig was filtered out. The merged Abyss assembly was reassembled using the 64-bit phrap version 1.080721 with the revise greedy option on a 16-core Intel Xeon 2.93 GHz server with 128 gigabytes DDR2 RAM. The phrap assembly resulted in a total of 1927 contigs with a median length of 2340 bp, and maximum and minimum lengths of 47,199 and 100 bp, respectively. The N50 contig length was 6593 bp, and 292 contigs were larger than this size. The contigs were matched to the reference *P. bryantii* genomic sequence using BLAT (16) at 99% identity. Transcriptome contigs, which matched more than one contig from the reference genome, were considered as potentially closing gaps in the partial genome sequence and were confirmed by PCR.

Cloning, Expression, and Purification of P. bryantii B₁₄ ORF0150, P. bryantii B₁₄ ORF0336, Bacteroides eggerthii ORF1299, B. intestinalis ORF1125, and B. intestinalis ORF4213—Genomic DNA was isolated from *P. bryantii* B₁₄ (13) and *B. intestinalis* DSM 17393 (17) using the DNeasy blood and tissue DNA purification kit. *B. eggerthii* DSM 20697 genomic DNA was a kind gift from Abigail A. Salyers (Department of Microbiology, University of Illinois, Urbana-Champaign). The DNA sequences for the five genes were amplified from genomic DNA using the PicoMaxx high fidelity PCR system with the oligonucleotide primers listed in supplemental Table S1. Putative signal sequences with corresponding cleavage sites were predicted for each of the five genes (PbORF0150, MNKKIIVCLA-CAISLSSMA; PbORF0336, MKKILAFIGSLLLLPMAALA; BeORF1299, MKNMKNTVSILLFLVFLSACS; BiORF4213, MKNNMRKIIYLLTLLGLVSLAACS; and BiORF1125, MKNITNVFYEFLLIALCCLMSSSTLWA) with the SignalP version 3.0 on-line server (18). To ensure that proteins accumulated within the cytoplasm of *E. coli* cells, the primers were engineered to clone the respective gene beginning with the amino acid just downstream of the predicted cleavage site.

The five genes were cloned into pET-46b by ligation-independent cloning as described previously (4). The recombinant hexahistidine proteins were expressed in *E. coli* BL21-Codon-Plus (DE3) RIL cells, and different purification schemes were used for each protein. For PbORF0150, the recombinant protein was purified by metal affinity chromatography using an ÄKTExpress instrument equipped with a HisTrap FF nickel column and a HiPrep 26/10 desalting column as described previously (4). For BeORF1299 and BiORF4213, the proteins were purified by metal affinity chromatography (HisTrap FF) followed by size exclusion chromatography (HiLoad 16/60 Super-

dex 200 column) with protein storage buffer (50 mM Tris-HCl, 150 mM NaCl (pH 7.5)) as the mobile phase. For PbORF0336 and BiORF1125, the proteins were purified by metal affinity chromatography using Talon resin from Clontech as described by the manufacturer followed by anion exchange chromatography (HiTrap Q XL) using the following binding and elution buffer pairs: PbORF0336, binding buffer, 50 mM Na₂HPO₄/NaH₂PO₄ (pH 8.0), and elution buffer, 50 mM Na₂HPO₄/NaH₂PO₄, 1 M NaCl, (pH 8.0); BiORF1125, binding buffer, 50 mM Na₂HPO₄/NaH₂PO₄ (pH 7.0) and elution buffer, 50 mM Na₂HPO₄/NaH₂PO₄, 1 M NaCl (pH 7.0). Fractions were analyzed by SDS-PAGE followed by staining with Coomassie Blue G-250. The purified protein concentrations were calculated using the method of Gill and von Hippel (19) with the following extinction coefficients: PbORF0150, 152.53 cm⁻¹ mM⁻¹; PbORF0336, 192.52 cm⁻¹ mM⁻¹; BeORF1299, 137.17 cm⁻¹ mM⁻¹; BiORF4213, 137.17 cm⁻¹ mM⁻¹; and BiORF1125, 294.17 cm⁻¹ mM⁻¹.

Evaluation of Xylanase Activity on Agar Plates—The hydrolytic activity of PbXyn5A with plant polysaccharides as substrate was assessed by using a Congo red-based assay adapted from Teather and Wood (20). The substrates were WAX, carboxymethyl cellulose, locust bean gum, or lichenan, each at 1% w/v.

Hydrolysis of Xylohexaose and Soluble Wheat Arabinoxylan—PbXyn5A (2 μM, final concentration) was incubated with xylohexaose (1% w/v, final concentration) in citrate buffer (50 mM sodium citrate, 150 mM NaCl (pH 5.5)) at 37 °C. At regular time intervals (0, 0.5, 1, 3, 5, 10, 20, 30, and 60 min). 1-μl aliquots were removed, and the products of hydrolysis were analyzed by TLC as described below.

To evaluate the capacity of PbXyn5A, BeXyn5A, and BiXyn5A to hydrolyze a longer polysaccharide chain such as xylan, each enzyme (0.5 μM, final concentration) was incubated with soluble wheat arabinoxylan (1% w/v) in citrate buffer (500 μl, final volume) at 37 °C. After 15 h, the concentration of reducing ends was estimated using the *para*-hydroxybenzoic acid hydrazide assay with glucose as the standard (21). For qualitative identification of the hydrolysis products, the reactions were resolved by TLC as described previously (9). For more quantitative analysis of the products of hydrolysis, the wheat arabinoxylan hydrolysates were analyzed by high performance anion exchange chromatography (HPAEC) as described earlier (4).

Site-directed Mutagenesis—Mutagenesis was performed by use of the QuikChange site-directed mutagenesis kit from Stratagene (La Jolla, CA). All the methods were as described in our earlier report (4). Furthermore, the expression and purification of the mutant recombinant proteins were performed as described above for the wild-type (WT) PbXyn5A, BeXyn5A, and BiXyn5A.

GenBank™ Accession Numbers—The genes listed in Fig. 1 and Table 3 are available on GenBank™ with the following accession numbers: ORF0150, HM454201.1; ORF0315, HM454202.1; ORF0316, HM454203.1; ORF0336, HM454200.1; ORF1114, HM454204.1; ORF1131, HM454205.1; ORF1893, CAB01855.1; ORF1906, HM454206.1; ORF1908, CAA89208.1; ORF1909, CAA89207.1; ORF1911, CAD21013.1; ORF1912, HM454207.1;

Xylan Degradation in the Bacteroidetes

ORF1917, ADD92015.1; ORF2001, HM454208.1; ORF2002, HM454209.1; ORF2003, HM454210.1; ORF2004, HM454211.1; ORF2350, HM454212.1; and ORF2351, HM454213.1.

RESULTS

Transcriptional Analysis of *P. bryantii* B₁₄ Using Microarrays and RNA-Seq—To assess the reproducibility of the microarray and RNA-Seq analyses, the expression levels for all annotated genes in the partial genome sequence of *P. bryantii* B₁₄ were compared for the two biological replicates using both technologies. These analyses revealed a high correlation in the expression level for each gene in the two biological replicates derived from either DNA microarray or RNA-Seq technologies (supplemental Fig. S1). These results suggest that the biological reproducibility in the gene expression levels was very high for both the microarray (WAX, $R^2 = 0.969$; XA, $R^2 = 0.977$) and RNA-Seq (WAX, $R^2 = 0.972$; XA, $R^2 = 0.932$) analyses.

To evaluate how well data derived from DNA microarrays and RNA-Seq analyses agree, the expression level for each gene was compared for each sample using both technologies. These results revealed that there was a positive correlation in the expression of genes identified using the two different techniques (supplemental Fig. S2); however, this correlation was moderate (WAX1, $R^2 = 0.649$; WAX2, $R^2 = 0.662$; XA1, $R^2 = 0.663$; and XA2, $R^2 = 0.568$). The moderate correlation between microarray and RNA-Seq analyses has been reported before, and it is predicted that this may arise due to the fact that microarrays lack sensitivity for genes expressed at low and high levels (22). Because of the reported higher dynamic range for gene expression using RNA-Seq, the subsequent analyses of transcriptional regulation focused on the results from the RNA-Seq experiments rather than the DNA microarray data.

The Illumina reads were assembled onto the reference genome for *P. bryantii* B₁₄, and a transcriptome map was generated for the bacterium during growth with each carbohydrate source. A representative transcriptome map is shown in supplemental Fig. S3 where the number of assembled reads for each nucleotide position within the genome is plotted on the inner circle. The most abundant reads mapped onto ribosomal RNA genes (16S and 23S), indicated by the most prominent peak on the transcriptome map and five of the smaller peaks. The high abundance of reads aligning to rRNA genes demonstrates that the removal of ribosomal RNA from the sample using the RiboMinus™ kit was incomplete. In addition to the ribosomal RNA genes, the other most highly expressed genes included genes important for housekeeping functions in the cell such as fatty acid biosynthesis (acyl carrier protein, ORF0076; FabF, ORF0077), ribosome biogenesis (small and large subunit ribosomal proteins as follows: ORF2542, ORF2216, ORF1370, ORF1137, ORF1214, ORF1368, ORF0740, ORF2553, ORF0177, ORF1421, and ORF1369), and glycolysis (fructose-bisphosphate aldolase, ORF2552; and glyceraldehyde-3-phosphate dehydrogenase, ORF2095) (supplemental Table S2).

Identification of Xylanolytic Genes Up-regulated at the Transcriptional Level during Growth of *P. bryantii* B₁₄ with WAX Compared with XA—During growth with WAX relative to XA, ~57 genes were induced greater than 4-fold, and 32 genes were repressed greater than 4-fold (Baggerly's test (15), $p < 0.05$)

TABLE 1

Genes induced greater than 4-fold during growth of *P. bryantii* B₁₄ with WAX as compared with XA assessed by RNA-Seq and listed by magnitude of induction^a

ORF	Annotation ^b	Fold change	P-value ^c	Signal sequence ^d
1894	hypothetical protein	402.56	1.25E-13	Yes
1905	putative outer membrane protein involved in nutrient binding (SusC)	371.44	3.10E-20	Yes
1893	endo-1,4-beta-xylanase A precursor	321.68	3.55E-27	Yes
2351	beta-xylosidase	314.24	3.50E-136	Yes
1895	putative outer membrane protein involved in nutrient binding (SusD)	300.94	5.73E-09	Yes
1896	putative outer membrane protein involved in nutrient binding (SusC)	249.31	4.86E-20	Yes
1897	putative outer membrane protein involved in nutrient binding (SusD)	228.19	1.66E-11	No ^e
2004	alpha-xylosidase	114.36	6.16E-34	Yes
1909	endo-1,4-beta-xylanase A precursor	113.41	2.10E-32	Yes
1908	beta-xylosidase / Alpha-N- arabinofuranosidase	78.05	2.18E-245	No
2350	maltodextrin glucosidase	77.92	2.12E-16	Yes
0150	hypothetical protein	53.53	1.24E-56	Yes
0336	hypothetical protein	30.32	8.89E-27	Yes
1910	GPH family transporter in unknown oligosaccharide utilization	30.29	6.70E-06	No
1911	putative secreted protein	30.1	2.37E-78	Yes
1928	hypothetical protein	24.73	2.35E-09	Yes
0284	conjunctive transposon protein TraE	21.65	1.03E-05	Yes
0096	hypothetical protein	20.54	7.03E-05	No
1906	possible beta-xylosidase, family 43 of glycosyl hydrolases	20.28	2.94E-279	Yes
2163	hypothetical protein	19.58	4.28E-08	Yes
1122	putative outer membrane protein involved in nutrient binding (SusC)	15.69	2.41E-55	Yes
2523	hypothetical protein	14.37	0.03	Yes
1927	hypothetical protein	13.84	1.08E-20	Yes
1917	glucan 1,4-beta-glucosidase	13.7	1.47E-46	Yes
0099	hypothetical protein	13.44	8.08E-04	Yes
2164	iron-regulated protein A precursor	13.03	2.79E-31	Yes
0101	hypothetical protein	12.59	1.82E-03	No
0316	endo-1,4-beta-xylanase D precursor	11.85	1.74E-211	Yes
1123	putative outer membrane protein involved in nutrient binding (SusD)	11.83	5.78E-57	Yes
1912	alpha-glucuronidase	9.54	1.17E-63	Yes
2003	xylosidase/arabinosidase	9.25	5.18E-06	Yes
1114	endo-1,4-beta-xylanase A precursor	9.2	1.35E-64	Yes
2165	lipoprotein, putative	9.03	2.04E-42	Yes
2527	hypothetical protein	7.49	3.85E-11	Yes
0285	hypothetical protein	7.37	0.05	No
0315	endo-1,4-beta-xylanase A precursor	7.35	1.15E-50	Yes
0282	Conjunctive transposon protein TraG	6.91	1.70E-04	Yes
2166	putative cytochrome C-type biogenesis protein	6.29	6.73E-04	Yes
1456	hypothetical protein	6.13	0.05	No
2316	hypothetical protein	6.05	0.04	No
0320	serine protease, subtilase family	5.93	0.03	No
2002	arabinan endo-1,5-alpha-L-arabinosidase	5.59	2.77E-15	Yes
0102	cell wall endopeptidase, family M23/M37	5.51	0.05	No
0322	putative outer membrane protein involved in nutrient binding (SusC)	5.17	0.02	Yes
0098	LtrC-like protein	5.14	9.11E-04	No
0097	hypothetical protein	5.12	1.20E-03	No
0286	DNA primase	5.1	0.04	No
0283	conjunctive transposon protein TraE	5.09	9.03E-07	Yes
1458	major outer membrane protein OmpA	4.57	1.01E-06	Yes
1131	hypothetical protein	4.39	6.35E-71	Yes
2465	xylulose kinase	4.35	5.32E-288	No
0323	lipoprotein, putative	4.35	3.48E-08	Yes
2001	maltodextrin glucosidase	4.28	4.60E-16	Yes
1939	hypothetical protein	4.1	4.72E-06	Yes
1941	ferrichrome-iron receptor	4.09	3.50E-04	Yes
1936	probable zinc protease pqqL	4.08	4.12E-06	Yes
1462	hypothetical protein	4.04	8.48E-03	Yes

^a *P. bryantii* B₁₄ was cultured in a synthetic medium with either soluble WAX or XA as the sole carbohydrate source. RNA was then extracted, and RNA-Seq experiments were performed as described under "Experimental Procedures."

^b Open reading frames were predicted, and annotations were assigned to the putative gene products using the RAST server (14). Genes located within the major xylanolytic gene cluster shown in Fig. 2 are indicated in boldface type.

^c Two-sided *p* values derived from Baggerly's test of the differences in means for two independent experiments are reported (15).

^d Signal peptides were predicted using the SignalP version 3.0 on-line server (18).

^e The predicted start codon of ORF1897 is just downstream of the beginning of a contig, and BLAST_p analyses revealed that close homologs of this protein possess N-terminal extensions, which suggested that this protein is truncated at the N terminus. Thus, the assignment of the absence of a signal peptide for this protein may not be accurate.

using RNA-Seq analysis (Tables 1 and 2). Annotation, based on predicted function, of the induced genes revealed that the majority code for hypothetical proteins, although GHs and membrane transporters, including starch utilization system (Sus) homologues, were also highly enriched. Additionally, a few genes with predicted functions in conjunctive transposition, protein degradation, and carbohydrate ester hydrolysis were also identified (Table 1). The GH genes that were highly

TABLE 2

Genes repressed greater than 4-fold during growth of *P. bryantii* B₁4 with WAX as compared with XA assessed by RNA-Seq and listed by magnitude of repression^a

ORF	Annotation ^b	Fold change	P-value ^c	Signal sequence ^d
0960	hypothetical protein	15.61	5.72E-03	Yes
0959	putative outer membrane protein (SusD homolog)	11.31	0.05	No
1551	putative outer membrane protein (SusC homolog)	7.72	2.29E-03	Yes
1862	hypothetical protein	6.95	0.02	Yes
1863	endo-arabinanase	6.92	2.01E-05	Yes
0958	putative outer membrane protein (SusC homolog)	6.29	4.15E-08	Yes
1094	putative outer membrane protein (SusD homolog)	5.75	0.02	Yes
2354	hypothetical protein	5.56	1.87E-02	No
0626	hypothetical protein	5.42	7.28E-04	No
2405	TraX family protein	5.34	7.93E-03	No
1898	beta-glucanase (GH43-GH88 two domain protein)	5.22	1.10E-08	Yes
1946	rhamnogalacturonan lyase	5.16	2.74E-04	Yes
1860	putative outer membrane protein (SusC homolog)	5.14	5.45E-09	Yes
1864	AraC family transcriptional regulator	5.07	0.03	No
2314	exo-poly-alpha-D-galacturonosidase	4.97	0.03	Yes
1558	hypothetical protein	4.87	4.87E-04	Yes
0667	endoglucanase B precursor (EC 3.2.1.4)	4.87	6.98E-03	No ^e
0632	putative outer membrane protein (SusD homolog)	4.86	6.38E-03	Yes
0419	hypothetical protein	4.67	0.03	Yes
1575	histidine decarboxylase	4.66	2.73E-03	Yes
1092	AraC family transcriptional regulator	4.64	0.04	No
1577	hypothetical protein	4.57	4.72E-05	No
1848	alpha-amylase (EC 3.2.1.1)	4.40	0.03	Yes
0611	hypothetical protein	4.36	9.97E-04	Yes
0191	hypothetical protein	4.35	0.02	Yes
1365	translation elongation factor G-related protein	4.32	0	No
0612	L-asparaginase (EC 3.5.1.1)	4.31	0.02	Yes
1234	putative outer membrane protein (SusD homolog)	4.31	0.03	Yes
1948	ABC transporter ATP-binding protein	4.21	0	No
1885	Putative polygalacturonase	4.21	0.05	Yes
0254	hypothetical protein	4.17	0.02	Yes
0487	hypothetical protein	4.05	0	Yes

^a *P. bryantii* B₁4 was grown in a synthetic medium with either WAX or XA as the sole carbohydrate source. RNA was then extracted, and RNA-Seq experiments were performed as described under "Experimental Procedures."

^b Open reading frames were predicted, and annotations were assigned to the putative gene products using the RAST server (14).

^c Two-sided *p* values derived from Baggerly's test of the differences in means for two independent experiments are reported (15).

^d Signal peptides were predicted using the SignalP version 3.0 on-line server (18).

^e The predicted start codon of ORF0667 is just downstream of the beginning of a contig, and BLASTp analyses revealed that close homologs of this protein possess N-terminal extensions, which suggest that this protein may be truncated at the N-terminus. Thus, the assignment of the absence of a signal peptide for this protein may not be accurate.

induced had predicted functions associated with the hydrolysis of xylan, including endoxylanases (five genes), β -xylosidases (four genes), and arabinofuranosidases (two genes). These results suggest that *P. bryantii* B₁4 elaborates a specific transcriptional response in the presence of xylan leading to induced expression of a subset of genes related to xylan degradation and utilization. Of the 57 induced genes, 77% code for proteins with putative signal sequences as predicted by using the SignalP server (Table 1) (18), suggesting that the metabolic repertoire induced during growth of *P. bryantii* B₁4 on WAX is polarized toward the periplasmic space or outer membrane.

To improve annotation of genes, which may encode xylanolytic enzymes, the 57 highly induced genes were analyzed using BLASTp to catalogue genes into different carbohydrate active enzyme (CAZy) families. Of the 57 highly induced genes, 19 clustered into CAZy families. Fourteen of the genes grouped into GH families, three grouped into carbohydrate esterase families, and two genes were predicted to encode polypeptides harboring both GH and carbohydrate esterase domains (Fig. 1). The most highly represented CAZy family in the subset of

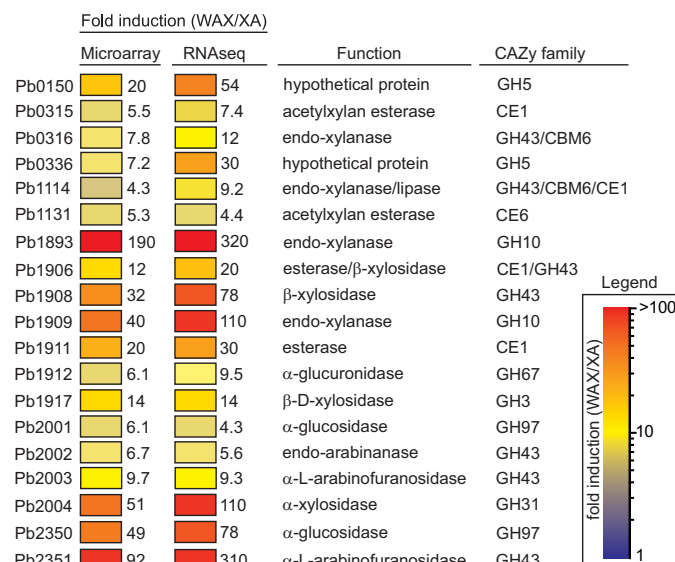


FIGURE 1. Carbohydrate esterase and glycoside hydrolase genes up-regulated on soluble WAX compared with XA. Each gene that was overexpressed at least 4-fold was used as a query in a BLASTp search of the non-redundant (*nr*) database at GenBankTM. Genes were assigned to CAZy (43) families if they exhibited significant similarity (E -value $< 1 \times 10^{-5}$) to biochemically characterized proteins already catalogued in a CAZy family. The GenBankTM accession numbers for these genes are listed under "Experimental Procedures."

induced genes was GH43 and the top six most highly induced genes included members from GH10 (ORF1893, ORF1909), GH31 (ORF2004), GH43 (ORF1908, ORF2351), and GH97 (ORF2350). The trends in these gene expression patterns were confirmed by both DNA microarray and RNA-Seq methods (Fig. 1).

The genes that were repressed during growth on WAX compared with XA were highly enriched for hypothetical genes and transporters (Table 2). The subset of glycoside hydrolase genes that were repressed had predicted functions associated with the depolymerization of polysaccharides such as arabinan, galacturonan, cellulose, and starch. Furthermore, SusC and SusD homologues were also found to be among the group of repressed genes. These results suggest that during growth on WAX, a transcriptional program is initiated that represses the expression of genes involved with degradation of non-xylan-containing polysaccharides.

Identification of the Major Xylanolytic Gene Cluster in P. bryantii B₁4—Five of the most highly induced genes clustered together near the edge of a single contiguous DNA sequence (contig 17) in the partial genome sequence of *P. bryantii* B₁4. The gene that was positioned closest to the end of the contig (ORF1897) appeared to be truncated at the N-terminal region relative to other homologous proteins within the GenBankTM database (data not shown). To evaluate whether the transcriptomic data may aid in completing the sequence for this highly expressed gene, a *de novo* assembly of the RNA-Seq data was carried out. Within the expressed sequence tag assembly, a large contig (expressed sequence tag contig 1388, 12,646 bp) was identified that exhibited overlap with the ends of two genomic DNA contigs (contig 17, 8656-bp overlap; contig 19, 3875-bp overlap). These data suggested that contigs 17 and 19 are closely positioned on the *P. bryantii* B₁4 chromosome and

Xylan Degradation in the Bacteroidetes

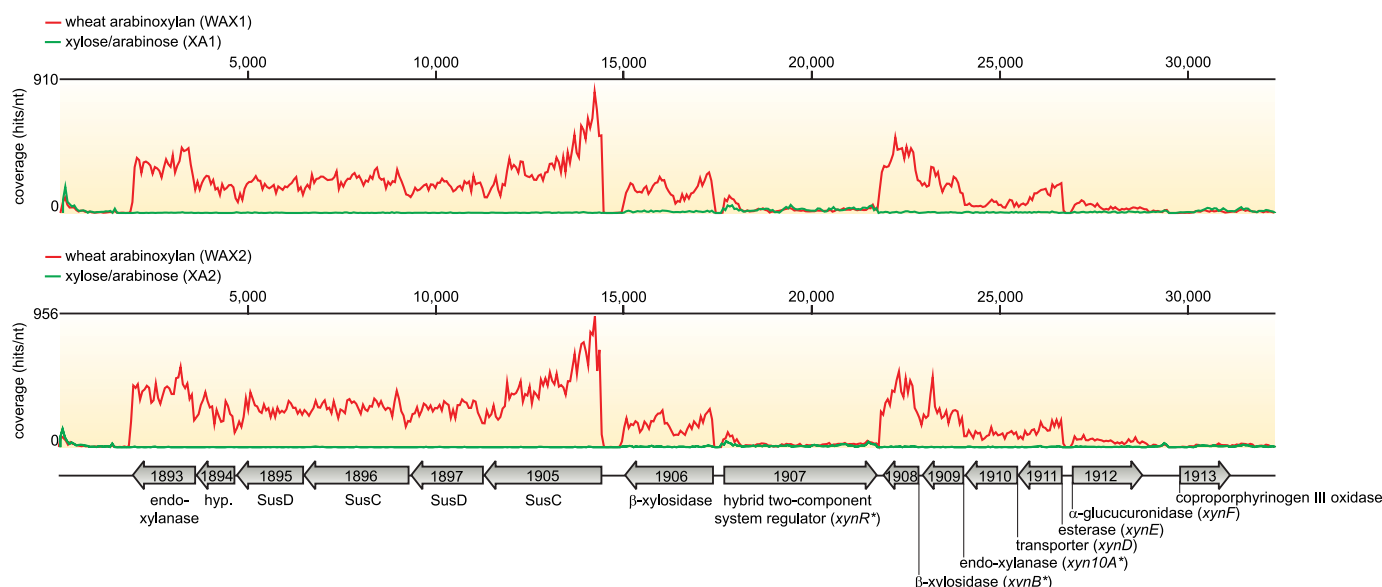


FIGURE 2. RNA-Seq coverage for the major xylanolytic gene cluster in *P. bryantii* B_{1,4}. *P. bryantii* B_{1,4} was grown with either WAX or a XA as the sole carbohydrate source, and the transcriptomes were analyzed by RNA-Seq as described under “Experimental Procedures.” A detailed view of the nucleotide coverage for the major xylanolytic gene cluster in *P. bryantii* B_{1,4} during growth on WAX (red) or XA (green) is shown for two biological replicates (WAX1, WAX2; XA1, XA2). The portion of the gene cluster including ORF1907–1912 has been studied previously by Flint and co-workers (7). Asterisks denote genes for which biochemical activities have been demonstrated for their cognate gene products: *xynB* and *xynA* (7) and *xynR* (5).

are separated by a 104-bp gap (supplemental Fig. S4). To test the results from this assembly, an oligonucleotide primer set was designed to amplify a 746-bp fragment that spans the predicted gap between the two genomic DNA contigs. Cloning and sequencing of the PCR fragment revealed that it indeed joins contigs 17 and 19, thus confirming the presence of a contiguous xylanolytic gene cluster on the *P. bryantii* B_{1,4} genome (Fig. 2).

Of the 20 most highly induced genes in *P. bryantii* B_{1,4}, 12 of them mapped to this major xylanolytic gene cluster (Table 1 and Fig. 2). Annotation of the genes identified a central gene (*xynR*, ORF1907) predicted to encode a hybrid two-component system regulator flanked by two groups of xylanolytic genes (Fig. 2). The genes upstream of *xynR* are divergently oriented and include a putative β -xylosidase/esterase (ORF1906) and an operon, which contained two pairs of *SusC*-*SusD* (ORF1905-ORF1897 and ORF1896-ORF1895) genes in tandem followed by a hypothetical protein (ORF1894), and then an endoxylanase gene (ORF1893, *xyn10C*). The genes downstream of *xynR* are also divergently oriented relative to *xynR* and include a putative β -xylosidase encoding gene (ORF1908, *xynB*) preceded by an endoxylanase gene (ORF1909, *xyn10A*), a sugar transporter encoding gene (ORF1910, *xynD*), and a putative esterase gene (ORF1911, *xynE*). Further downstream from this cluster relative to *xynR* is a putative α -glucuronidase gene (ORF1912, *xynF*), which is in the same orientation as *xynR*. The RNA coverage or expression of each gene in the cluster was higher for the WAX-grown cultures relative to the XA-grown cultures except for *xynR* and ORF1913 (Fig. 2).

The RNA coverage was continuous throughout ORF1911-ORF1908, which is highly suggestive that these four genes are co-transcribed within a single messenger RNA molecule (Fig. 2). Furthermore, the RNA coverage is continuous throughout ORF1905-ORF1893, which suggests that these six genes are also co-transcribed within a single mRNA molecule (Fig. 2).

The observed differences in the RNA coverage, e.g. ORF1908 and ORF1909 versus ORF1910 and ORF1911, may also indicate that there are multiple promoter elements present within this cluster and that the RNA coverage represents the presence of mRNA molecules with different 5' ends. Another notable fluctuation in coverage occurred within the genes, ORF1906 and ORF1905. These fluctuations were observed in both of the biological replicates (WAX1 and WAX2), which provides evidence that the observed patterns in RNA coverage were reproducible. The intragenic variations in coverage, such as that observed with ORF1905, may reflect different susceptibilities of regions within the transcripts to degradation by native endoribonuclease enzymes.

P. bryantii B_{1,4} ORF0150 Encodes a Glycoside Hydrolase Family 5 Endoxylanase—Of the 57 genes that were induced greater than 4-fold during growth on WAX relative to XA, 18 were predicted to code for hypothetical proteins, according to the RAST server and a GenBank™ database search (Table 1). Further analysis showed that two of the genes (ORF0150 and ORF0336) exhibited homology at the amino acid level to each other (50% identity, 415 residues aligned) and also low homology to enzymes from the glycoside hydrolase family 5. The gene for ORF0150 was selected for further analysis, because this gene was more highly induced on WAX relative to XA in the transcriptional study. For ORF0150, the most similar enzyme with a biochemically defined function in the GenBank™ database is the alkaline endoglucanase enzyme from *Bacillus* sp. KSM-635 (23), although the amino acid conservation between these two proteins is low (27% identity over 207 amino acids aligned). These results suggested that ORF0150 encodes a glycoside hydrolase, and the likely group is GH family 5. To test this possibility, the recombinant hexahistidine fusion protein, with a predicted molecular mass of 79 kDa, was made in *E. coli* cells and purified (Fig. 3A). Enzymatic activity was then tested with

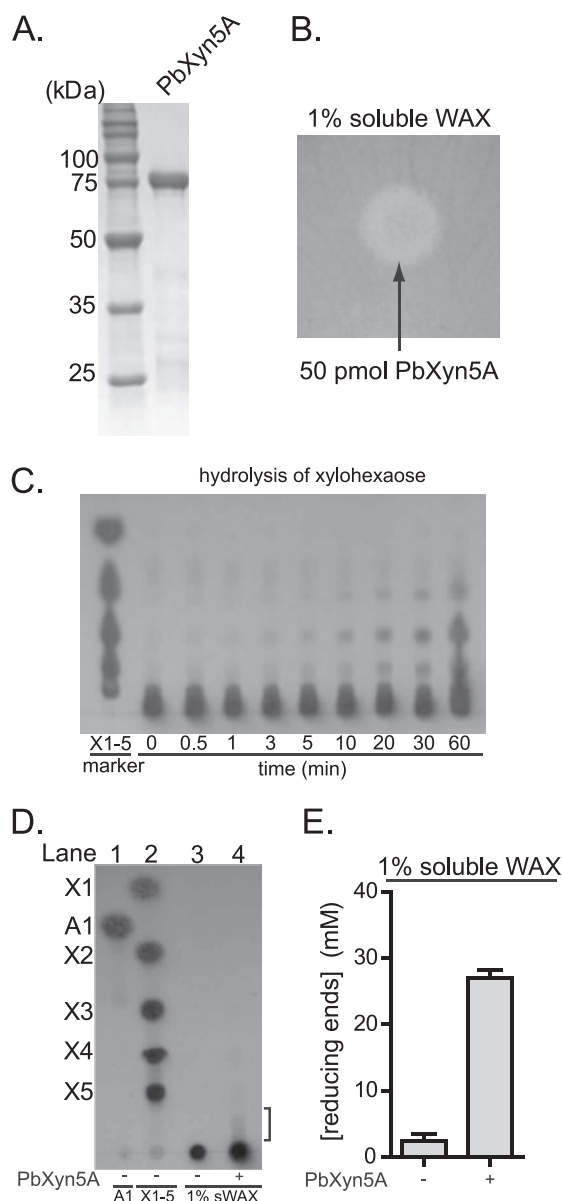


FIGURE 3. *P. bryantii* B₄ ORF0150 encodes an enzyme with endoxylanase activity. *A*, purification of recombinant PbXyn5A. ORF0150 was cloned into an expression vector and expressed heterologously as a hexahistidine fusion protein in *E. coli*. The protein (PbXyn5A) was purified using cobalt affinity chromatography, and the eluate was analyzed by 12% SDS-PAGE, followed by Coomassie Brilliant Blue G-250 staining. *B*, depolymerization of soluble wheat arabinoxylan. PbXyn5A was assessed for its capacity to depolymerize soluble WAX by incubating the protein on an agar plate infused with WAX followed by staining and destaining with Congo red and 1 M NaCl, respectively. *C*, hydrolysis of xylohexaose. PbXyn5A-catalyzed hydrolysis of xylohexaose was assessed by incubating the enzyme with the substrate, removing aliquots at the indicated time points, and then resolving the products by thin layer chromatography followed by staining with methanolic orcinol. *D*, thin layer chromatography of products released from WAX by PbXyn5A. PbXyn5A (0.50 μ M) was incubated with WAX (1% w/v), and the products were resolved by thin layer chromatography followed by staining with methanolic orcinol. Xylo-oligosaccharide standards X₁–X₅ and arabinose (A1) were spotted on the plate in lanes 2 and 1, respectively, to serve as markers for the identification of hydrolysis products. In lane 4, PbXyn5A was incubated with WAX at 37 °C for 15 h, and 2.5 μ l of the reaction mixture were resolved on the TLC plate. *E*, reducing sugars released from WAX by PbXyn5A. Wild-type Xyn5A was incubated with WAX (1% w/v), and the amounts of reducing sugars released were determined by the *para*-hydroxybenzoic acid hydrazide assay. The reducing sugar concentrations were calculated from the absorbance at 410 nm by comparison to a standard curve generated with known concentrations of glucose. *E*, the values are reported as the means \pm S.D. from three independent experiments.

WAX, carboxymethyl cellulose, locust bean gum, or lichenan as substrates using an agar plate assay. A zone of Congo red exclusion, representing hydrolysis of WAX was observed (Fig. 3*B*). In contrast, clearing zones were not seen on the plates containing carboxymethyl cellulose, locust bean gum, or lichenan. These results suggested that the gene product of ORF0150 possesses xylanase activity but not endoglucanase, mannanase, or lichenanase activities. Because this gene encodes the first GH family 5 endoxylanase identified in *P. bryantii* B₄, it was designated *xyn5A*.

To further verify the endoxylanase activity of PbXyn5A, the enzyme was incubated with xylohexaose, and aliquots of end products were removed at specific time intervals and analyzed by TLC. Products corresponding to xylobiose, xylotriose, and xylo-tetraose accumulated in the reaction mixture (Fig. 3*C*), thus supporting assignment of endoxylanase activity to PbXyn5A. The sizes of products released from WAX by Xyn5A were resolved by TLC, and the amounts of reducing ends released were also determined. In the absence of the enzyme, no depolymerization of the substrate was evident (Fig. 3*D*, lane 3). However, when the enzyme was incubated with the substrate, a smear of oligosaccharides was apparent near the bottom of the TLC plate (Fig. 3*D*, lane 4). Furthermore, the concentration of reducing sugars in the reaction mixture increased \sim 9-fold following the addition of PbXyn5A (Fig. 3*E*), indicating depolymerization of the xylan substrate. The results therefore suggested that PbXyn5A releases long oligosaccharides from WAX and that the products are not clearly resolved by TLC.

To evaluate whether PbXyn5A exhibits synergistic activity with other xylanolytic enzymes, it was incubated independently or in combination with an α -L-arabinofuranosidase (Ara43A) and a β -D-xylosidase (Xyl3B) in the presence of WAX, and the products of hydrolysis were resolved by HPAEC. Injection of xylo-oligosaccharide (X₂–X₆) standards allowed determination of retention times for identification of end products of hydrolysis. The concentrations of xylose and arabinose in the reaction mixtures were determined by comparison of the peak areas with standard curves generated with known concentrations of xylose or arabinose. The enzyme, Ara43A, is a GH family 43 arabinoxylan arabinofuranohydrolase from *P. bryantii* B₄, encoded by ORF2351, and was cloned and expressed in our laboratory.³ Xyl3B is a GH family 3 β -D-xylosidase from *P. bryantii* B₄, and it releases xylose from xylo-oligosaccharides (4). In the absence of all enzymes, neither monomers nor oligosaccharides were detectable in the substrate (Fig. 4). When WAX was incubated with Ara43A, a sizeable amount of arabinose was detected (Fig. 4*A*). When WAX was incubated with Xyl3B, small amounts of arabinose and xylose were detected (Fig. 4*A*). The release of both xylose and arabinose by Xyl3B is consistent with previous results which demonstrated activity with both *para*-nitrophenyl (*p*NP) α -L-arabinofuranoside and *p*NP- β -D-xylopyranoside (4). When WAX was incubated with PbXyn5A, no monosaccharides were detected (Fig. 4*A*); however, several peaks that eluted after the retention times for xylobiose were observed (Fig. 4*B*), which suggests that these peaks represent

³ S. Kiyonari, Y.-H. Moon, D. Dodd, R. I. Mackie, and I. K. O. Cann, manuscript in preparation.

Xylan Degradation in the Bacteroidetes

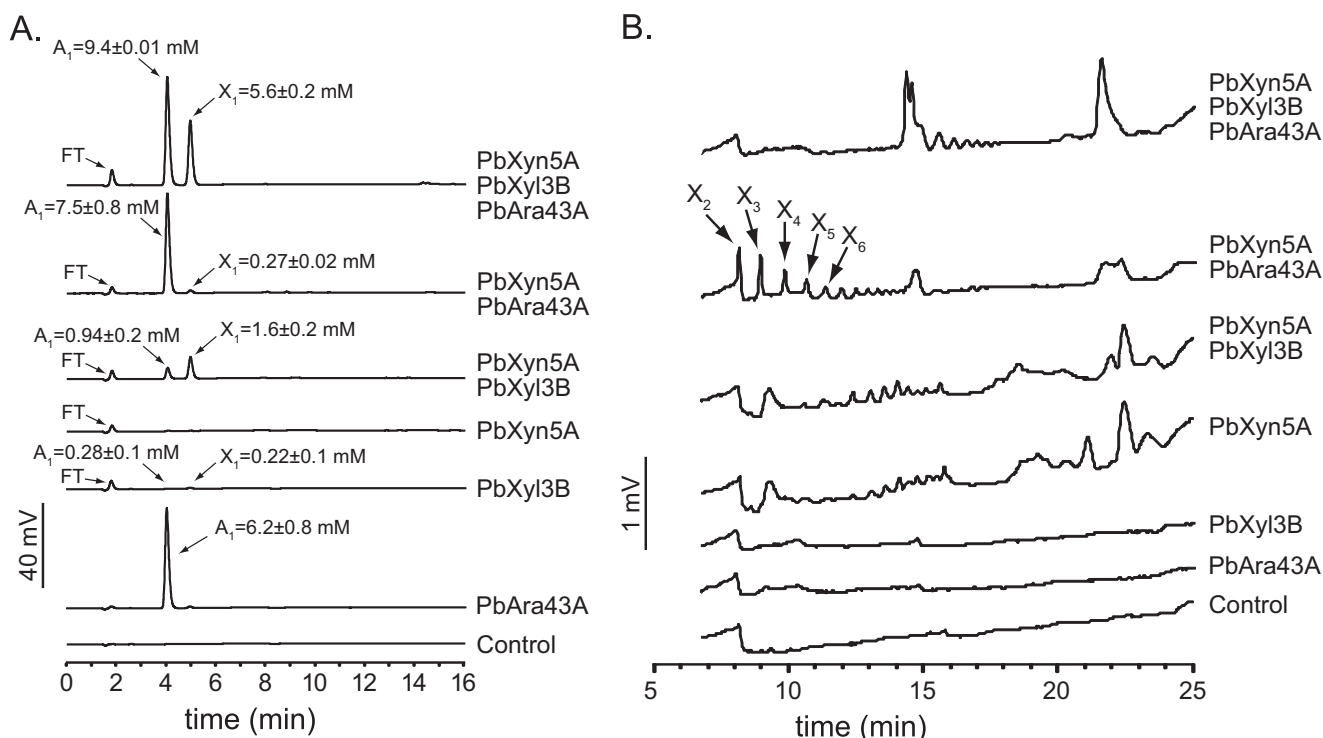


FIGURE 4. PbXyn5A functions synergistically with β -xylosidase and α -L-arabinofuranosidase enzymes. A and B, hydrolysis of WAX was assessed by incubating the respective enzymes with the substrate and then resolving the products by HPAEC followed by detection with a pulsed amperometric detector. The products of hydrolysis were identified by comparison of peaks with retention times of purified substrates. Abbreviations are as follows: FT, flow-through; A_1 , arabinose; X_1 – X_6 , xylose through xylohexaose. The concentration of xylose and arabinose in each of the reactions was estimated by a calibration curve constructed with known concentrations of each sugar. The same chromatograms are depicted in A and B; however, the scale is adjusted in B to reveal changes in the oligosaccharide patterns between different reactions. These experiments were performed three times, and single representative curves are shown. The concentrations of xylose and arabinose are reported as means \pm S.D.

xylo-oligosaccharide fragments that are either longer than our standards or are decorated with arabinose. Incubation of WAX with both PbXyn5A and Xyl3B resulted in an increase in the release of xylose and arabinose over either PbXyn5A or Xyl3B alone (Fig. 4A). When PbXyn5A and Ara43A were incubated together with WAX, the concentrations of xylose and arabinose were similar as compared with Ara43A alone (Fig. 4A); however, the pattern of xylo-oligosaccharides was different compared with PbXyn5A alone with peaks appearing that exhibited similar retention times to the xylo-oligosaccharide standards (X_2 – X_6) (Fig. 4B). These data revealed that PbXyn5A and Ara43A do not exhibit synergism in the release of xylose or arabinose, but they do exhibit synergism in the release of xylo-oligosaccharides. When all three enzymes were incubated together, the amount of xylose released was increased relative to each of the other enzyme combinations, whereas the level of arabinose was similar to Ara43A alone. Moreover, no peaks corresponding to the xylo-oligosaccharide standards were identified. These experiments revealed that PbXyn5A is an endoxylanase that functions synergistically with a β -D-xylosidase/ α -L-arabinofuranosidase and an arabinofuranohydrolase from the same bacterium to release xylose from WAX.

B. eggerthii ORF1299 and *B. intestinalis* ORF4213 Each Encode Glycoside Hydrolase Family 5 Endoxylanases—A BLASTp search of the GenBank™ nonredundant (nr) database using PbXyn5A as the query revealed that the most closely related proteins derive from members of the human colonic Bacteroidetes (Table 3). These proteins do not have biochemi-

TABLE 3
Domain architecture for ORF0150 from *P. bryantii* B₁4 and its top BLAST hits

Source (ORF, GenBank accession no.)	Domain architecture ^a	Predicted activity	Amino acid identity ^b	No. of amino acids aligned
<i>Prevotella bryantii</i> B ₁ 4 (ORF0150, HM454201.1)	GH 5	hypothetical protein	-	-
<i>Prevotella copri</i> (ORF6092, ZP_06253187)	GH 5	cellulase	52%	433
<i>Prevotella bryantii</i> B ₁ 4 (ORF0336, HM454200.1)	GH 5	hypothetical protein	50%	415
<i>Prevotella buccae</i> D17 (ORF1726, ZP_06420215)	GH 5	hypothetical protein	49%	414
<i>Prevotella ruminicola</i> 23 (ORF2706, YP_003575953)	GH 5	endoglucanase precursor	46%	519
<i>Prevotella buccae</i> D17 (ORF0844, ZP_06419333)	GH 5	hypothetical protein	35%	686
<i>Bacteroides</i> sp. 2_2_4 (ORF3750, ZP_04550243)	GH 5, Ig2	hypothetical protein	35%	665
<i>Bacteroides cellulosilyticus</i> (ORF3415, ZP_03679060)	GH 5, Ig2	hypothetical protein	35%	657
<i>Bacteroides intestinalis</i> (ORF4213, ZP_03016606)	GH 5, Ig2	hypothetical protein	34%	657
<i>Bacteroides eggerthii</i> (ORF1299, ZP_03458524)	GH 5, Ig2	hypothetical protein	35%	664
<i>Bacteroides intestinalis</i> (ORF1125, ZP_03013566)	GH 5, GH 43	hypothetical protein	34%, 31%	434, 316
<i>Bacteroides cellulosilyticus</i> (ORF2048, ZP_03677110)	GH 5, GH 43	hypothetical protein	34%, 28%	434, 428

^a Functional domains were assigned utilizing the Conserved Domain Database on the NCBI database (www.ncbi.nlm.nih.gov). The regions of the polypeptides were selected as belonging to a domain if the expected value (*E*-value) for the protein query compared with the consensus sequence generated for the particular domain was less than or equal to 0.01.

^b Amino acid identities are shown for each open reading frame derived from alignments with *P. bryantii* ORF0150. For *B. intestinalis* ORF1125 and *B. cellulosilyticus* ORF2048, the amino acid sequence alignments with *P. bryantii* ORF0150 were discontinuous with similarity occurring at the N and C termini but with no significant similarity at the regions predicted to code for the GH 43 domain. Correspondingly, two amino acid identity values are provided that correspond to alignment with *P. bryantii* ORF0150 at the N and C termini, respectively.

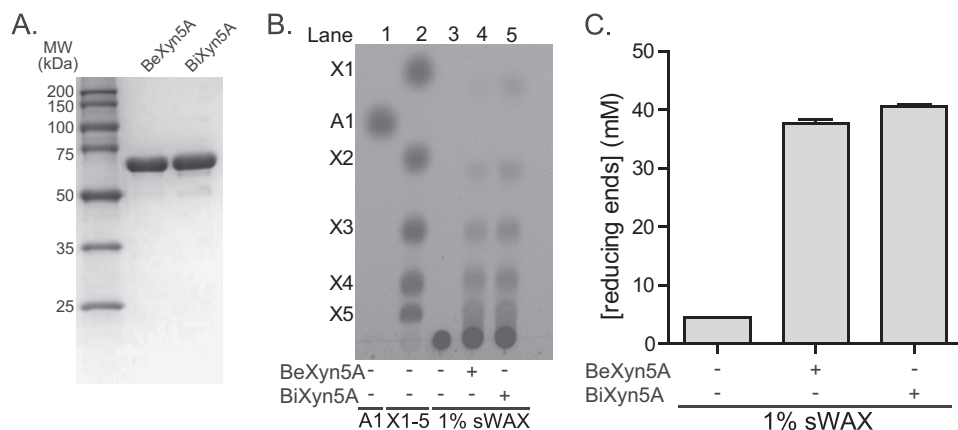


FIGURE 5. *B. eggerthii* ORF1299 and *B. intestinalis* ORF4213 encode endoxylanases. A, purification of recombinant BeXyn5A and BiXyn5A. B, *B. eggerthii* ORF1299 and *B. intestinalis* ORF4213 were cloned into expression vectors and expressed heterologously as hexahistidine fusion proteins in *E. coli*. The proteins were purified using cobalt affinity chromatography and gel filtration, and the elution fractions were pooled and analyzed by 12% SDS-PAGE, followed by Coomassie Brilliant Blue G-250 staining. B, thin layer chromatography of products released from WAX by BeXyn5A and BiXyn5A. BeXyn5A or BiXyn5A (0.50 μ M each) was incubated with WAX (1% w/v) for 15 h at 37 °C, and the products were resolved by thin layer chromatography followed by staining with methanolic orcinol. Xylo-oligosaccharide standards X₁–X₅ and arabinose (A1) were spotted on the plate in lanes 2 and 1, respectively, to serve as markers for the identification of hydrolysis products. C, reducing sugars released from sWAX by BeXyn5A and BiXyn5A. BeXyn5A or BiXyn5A (0.50 μ M each) was incubated with WAX (1% w/v) for 15 h at 37 °C, and the reducing sugars were detected by using the *para*-hydroxybenzoic acid hydrazide assay. The reducing sugar concentrations were calculated from the absorbance at 410 nm by comparison with a standard curve generated with known concentrations of glucose. C, the values are reported as the means \pm S.D. from three independent experiments.

cally defined functions; therefore, to assess whether they also encode endoxylanases, the *B. eggerthii* DSM20697 ORF1299 and *B. intestinalis* DSM17393 ORF4213 were expressed for biochemical characterization. The recombinant hexahistidine fusion proteins were purified by metal affinity chromatography. The predicted molecular masses for his-BeXyn5A and his-BiXyn5A were 72 and 73 kDa, respectively, and the sizes of the purified proteins, estimated by SDS-PAGE, were in agreement (Fig. 5A). Both the TLC and reducing sugar assays showed that the two enzymes can depolymerize WAX. In the absence of either enzyme, no depolymerization of the substrate was evident (Fig. 5B, lane 3); however, when the enzymes were independently incubated with the substrate, oligosaccharides were released (Fig. 5B, lanes 4 and 5). For both BeXyn5A and BiXyn5A, several spots, including those that migrated to similar distances as xylotriase and xylo-tetraose, were observed on the TLC plate (Fig. 5B, lanes 4 and 5). Furthermore, these two enzymes released large amounts of reducing sugars from WAX (Fig. 5C). Taken together, these results revealed that both BeXyn5A and BiXyn5A are endoxylanases.

To provide insight into the products that are released from WAX by BeXyn5A and BiXyn5A, and to evaluate whether these enzymes also function synergistically with Ara43A and Xyl3B, the enzymes were incubated alone or in combination with Ara43A and Xyl3B, and the hydrolysates were analyzed by HPAEC. The patterns of hydrolysis for Ara43A and Xyl3B were identical to that described above (Fig. 4A). Following incubation of WAX with BeXyn5A, arabinose was released (Fig. 6A), and a mixture of oligosaccharides, including xylobiose and xylo-tetraose, was also detected (Fig. 6B). Incubation of WAX with both BeXyn5A and Xyl3B resulted in an increase in the concentration of xylose over either BeXyn5A or Xyl3B alone (Fig. 6A), and the oligosaccharide pattern was different from

BeXyn5A alone (Fig. 6B). Incubation of both BeXyn5A and Ara43A with WAX released arabinose at a concentration that was higher than the sum of each enzyme acting alone (Fig. 6A), and xylo-oligosaccharides (X₂–X₆) were clearly visible (Fig. 6B). These results demonstrate that BeXyn5A functions synergistically with Xyl3B to release xylose from WAX. In addition, BeXyn5A and Ara43A function synergistically to release arabinose and xylo-oligosaccharides from WAX. The data also show that BeXyn5A releases both oligosaccharides and arabinose from WAX, indicating that this enzyme has both endoxylanase and arabinofuranosidase activities.

When BiXyn5A was incubated with WAX, no monosaccharides were released (Fig. 6C). However, larger oligosaccharides were detected in the hydrolysates, and these

included xylobiose and xylo-tetraose (Fig. 6D). Incubation of WAX with both BiXyn5A and Xyl3B resulted in an increase in the concentration of xylose over either BiXyn5A or Xyl3B alone (Fig. 6C), and the oligosaccharide pattern was different from BiXyn5A alone, with no xylobiose or xylo-tetraose being detected (Fig. 6D). The level of arabinose released by BiXyn5A and Ara43A in combination was similar to Ara43A alone (Fig. 6C); however, in the presence of both enzymes, xylo-oligosaccharides (X₂–X₆) were released (Fig. 6D). This indicated that BiXyn5A functions synergistically with Ara43A to improve the release of unbranched xylo-oligosaccharides; however, no synergism was observed between the two enzymes in the release of arabinose. These results confirmed that *B. intestinalis* ORF4213 encodes an endoxylanase.

Although both BeXyn5A and BiXyn5A have endoxylanase activity, the oligosaccharide patterns in their hydrolysates differed. Moreover, BeXyn5A releases almost twice the amount of arabinose and xylose when co-incubated with Ara43A and Xyl3B relative to BiXyn5A. This observation clearly showed that although the two enzymes encode endoxylanases within the same GH family and also have similar domain organization (Table 3), they release different products from soluble wheat arabinoxylan.

Mutational Analyses Reveal Conserved Active Site Residues in PbXyn5A, BeXyn5A, and BiXyn5A—To further test the prediction that these three enzymes are GH family 5 enzymes and that they employ a similar mechanism for hydrolysis as other biochemically characterized GH5 enzymes, we probed for conserved amino acid sequence motifs by using position-specific iterative BLAST (PSI-BLAST) (24). This analysis revealed the presence of two amino acid sequence motifs that contained the putative glutamic acid catalytic acid/base (supplemental Fig. S5A, motif 2) and the putative glutamic acid catalytic nucleo-

Xylan Degradation in the Bacteroidetes

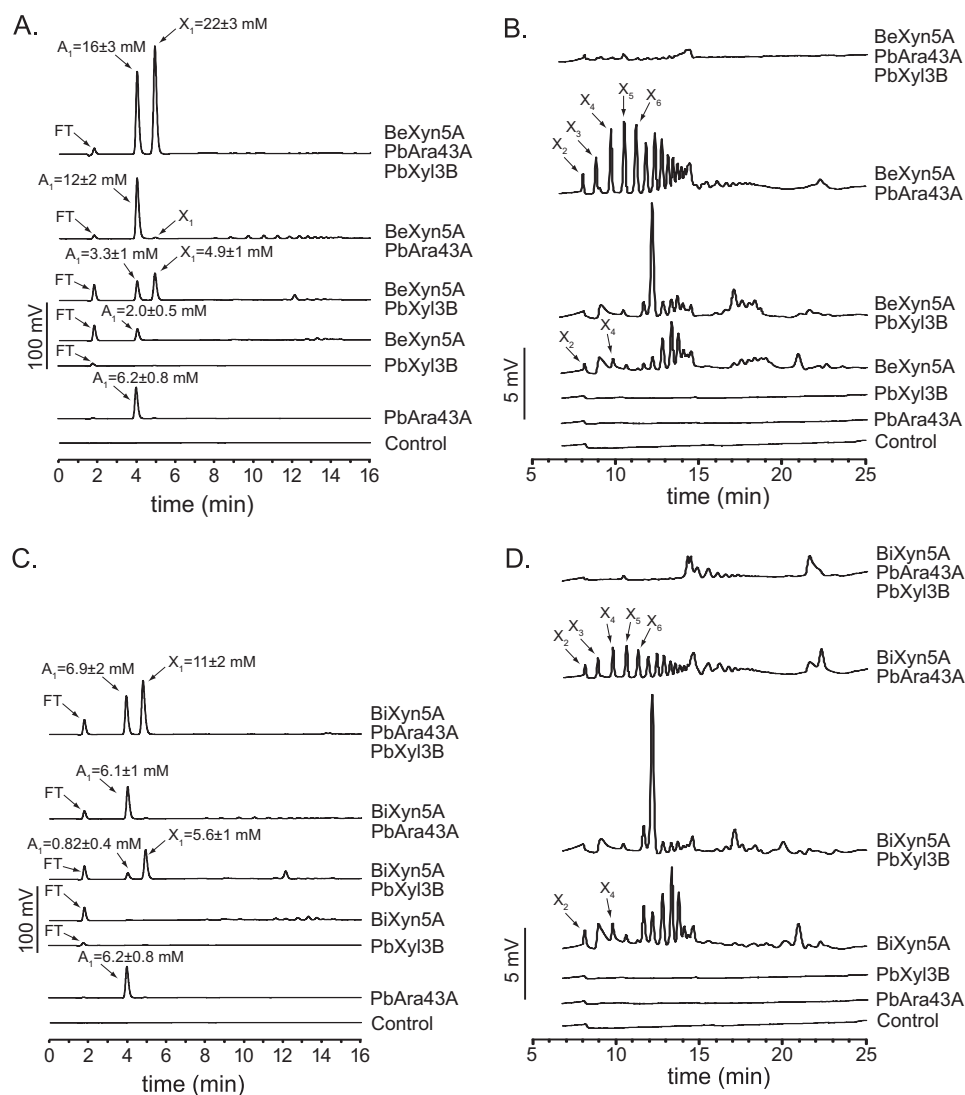


FIGURE 6. BeXyn5A and BiXyn5A release long xylo-oligosaccharides from WAX. A–D, hydrolysis of wheat arabinoxylan was assessed by incubating the enzymes with WAX (1% w/v) and then resolving the products by HPAEC followed by detection with a pulsed amperometric detector. The products of hydrolysis were identified by comparison of peaks with retention times of purified substrates. Abbreviations are as follows: FT, flow-through; X_2 , xylobiose; X_3 , xylotriose; X_4 , xylo-tetraose; X_5 , xylo-pentaose; X_6 , xylo-hexaose. The concentration of xylose and arabinose in each of the reactions was estimated by comparison with a calibration curve constructed with known concentrations of each sugar. The same chromatograms are depicted in A and B as well as in C and D; however, the scale is adjusted in B and D to reveal changes in the oligosaccharide patterns between different reactions. These experiments were performed three times, and single representative curves are shown. The concentrations of xylose and arabinose are reported as means \pm S.D.

phile (supplemental Fig. S5A, motif 3). An additional motif was identified (supplemental Fig. S5A, motif 1) that contained an aspartic acid in PbXyn5A, BeXyn5A, and BiXyn5A that aligned with a conserved tyrosine residue that was shown to make contact with the cellobiose ligand in the crystal structure for the alkaline cellulase K from *Bacillus* sp. strain KSM-635 (25). On mutating each of the three residues (PbXyn5A D104A, PbXyn5A E203A, PbXyn5A E308A, BeXyn5A D129A, BeXyn5A E229A, BeXyn5A E349A, BiXyn5A D127A, and BiXyn5A E227A and E347A), only the mutations that targeted the glutamic acid residues abolished catalysis (supplemental Fig. S5, B and C). This finding was further evidence that the three proteins belong to GH family 5, because the data suggest that they employ similar amino acid residues in catalysis as described for GH5 enzymes (25).

DISCUSSION

Xylans are an abundant group of plant polysaccharides that are hydrolyzed and fermented by commensal microbes within the rumen (26–28) and the human gut (29–35). Despite the abundance of xylanolytic bacteria in these microbiomes, relatively little is known about the mechanisms underlying the degradation and utilization of xylan by these bacteria.

In this study, a whole genome transcriptomic approach was employed to evaluate the repertoire of genes that the rumen hemicellulolytic bacterium *P. bryantii* B₁₄ employs to degrade xylan. The regulation of xylanase activity has been studied previously in *P. bryantii* B₁₄, and it was found that xylanase activity is not induced by glucuronic acid, arabinose, xylose, or small xylo-oligosaccharides (X_2 – X_5) (12). Rather, the major inducers of xylanase activity were found to be medium to large sized xylo-oligosaccharides. Our data confirmed the results from this previous study and reveal that the two previously studied endoxylanase genes (*xyn10A* and *xyn10C*) are highly induced during growth on soluble WAX compared with the component monosaccharides, XA. Although these genes were among the top 10 most highly induced genes, a large number of additional genes were also induced under these conditions. This observation underscores the complexity in the transcriptional response of *P. bryantii* B₁₄ during growth on this arabinoxylan polysaccharide.

The major xylanolytic gene cluster in *P. bryantii* B₁₄ identified in this study contains a genomic DNA fragment that was previously cloned by Gasparic *et al.* (7). The genes previously identified include open reading frames 1907 (*xynR*), 1908 (*xynB*), 1909 (*xyn10A*), 1910 (*xynD*), 1911 (*xynE*), and 1912 (*xynF*), although our data suggest that two genes (*xynR* and *xynF*) on either end of the DNA fragment reported by Gasparic *et al.* (7) were truncated in their study. A translation start site (ATG) that occurs 1602 bp upstream of the start site predicted for this gene by Gasparic *et al.* (7) was identified for *xynR* (ORF1907), and the assignment of this alternative start site was corroborated by the RNA-Seq coverage, which is continuous throughout the entire length of ORF1907 (Fig. 2). This result suggests that the xylan catabolism regulator (XynR) in *P. bryantii* B₁₄ is

534 amino acids longer than originally reported. Analysis of the domain architecture for this protein revealed three functional domains, including a putative N-terminal periplasmic sensing domain, followed by a histidine kinase domain and a response regulator domain (supplemental Fig. S6). Thus, this hybrid two-component system regulator contains all of the regulatory elements found in “classical” two-component regulatory systems, but rather than encoding the sensor and effector domains in separate genes as in the classical system, *xynR* encodes all of these functions within a single polypeptide. The domain organization for XynR is analogous to that for a hybrid two-component system regulator (BT3172) characterized from the related bacterium, *Bacteroides thetaiotaomicron* VPI-5482 (36); however, the sequence similarity across the entire polypeptide is relatively low (23%, 1405 amino acids aligned). The gene *xynR* was shown to be important for coordinating the transcription of a xylan utilization gene cluster in response to growth on xylan in *P. bryantii* B₁₄ (5); thus, this protein may be the primary regulator responsible for the transcriptional response identified in this study. This hypothesis can be tested by constructing a *P. bryantii* B₁₄ strain carrying a deletion in this gene and examining its growth on xylan. However, the lack of a genetic system for manipulating *P. bryantii* B₁₄ precludes this analysis at the current time. The gene *xynR* is conserved in the human colonic xylan utilizing bacterium *Bacteroides ovatus*, which is amenable to genetic manipulation. Thus this bacterium can be used as a model to investigate the role of the hybrid two-component system in the catabolism of xylan.

The xylan utilization gene cluster previously characterized by Gasparic *et al.* (7) was found to be part of a larger xylanolytic gene cluster that includes the previously characterized endoxylanase gene, *xyn10C* (10). The gene for Xyn10C (ORF1893) occurs in a group of six genes that the RNA-Seq data suggest are co-transcribed within a single polycistronic mRNA molecule. This operon includes six of the seven most highly induced genes during growth on WAX relative to XA, which indicates that it is likely to be of critical importance to xylan utilization by *P. bryantii* B₁₄. Contained within this operon are two tandem repeats of genes predicted to encode outer membrane proteins that share homology to the starch utilization system (Sus) components, SusC and SusD, followed by a hypothetical gene that is then followed by *xyn10C*. This arrangement of genes is similar in certain respects to the starch utilization system identified by Salyers and co-workers (37) in *B. thetaiotaomicron*. SusC is predicted to encode an outer membrane porin that transports oligosaccharides into the periplasm in a TonB-dependent fashion. SusD harbors a signal peptidase II cleavage site that may facilitate the tethering of this protein onto the outer leaflet of the outer membrane where it may play a role in oligosaccharide binding (38). The hypothetical protein (ORF1894) and Xyn10C both possess putative signal peptidase II cleavage sites, which suggests that these two proteins are also tethered on the outer surface of the cell. The function of the hypothetical protein (ORF1894) has yet to be determined; however, its location within this highly induced xylan utilization operon suggests that it is involved in the degradation and utilization of xylan. The gene product has been made and purified, and when tested it exhibited a zone of Congo red exclusion following incubation

on a WAX-infused agar plate (data not shown). Analysis of the activity of this protein is an ongoing focus in our laboratory. These observations suggest that this cluster of six proteins may be critical for the binding, depolymerization, and transport of extracellular xylan fragments into the periplasmic space, although further functional studies must be performed to verify this hypothesis.

The arrangement of this operon is conserved among a number of bacteria for which genome sequences are available, including *Prevotella ruminicola*, *Prevotella copri*, *Prevotella buccae*, *Prevotella bergensis*, *B. intestinalis*, *Bacteroides cellulosilyticus*, *Bacteroides* sp. 2_2_4, *B. ovatus*, *B. eggerthii*, *Bacteroides plebeius*, and an additional Bacteroidetes member, *Spirosoma linguale* that is commonly isolated from soil or freshwater (Fig. 7 and supplemental Fig. S7). These organisms are members of the phylum Bacteroidetes and, with the exception of *S. linguale*, they were isolated from the bovine rumen or the human alimentary tract (supplemental Fig. S7). This is the first evidence of a xylan utilization cluster that is strictly conserved across xylan degrading members of the rumen *Prevotella* and the human-associated *Bacteroides* spp. The conservation of this cluster is highly suggestive that xylanolytic members from these two bacterial genera employ a conserved mechanism to degrade and utilize xylan. Apart from the high level of conservation in the orientation of genes within this operon, there are no other strictly conserved arrangements of genes in the regions nearby on the chromosome (Fig. 2). It has been proposed that the Sus system, initially identified by Salyers and co-workers (37, 39), represents a paradigm for oligo- and polysaccharide utilization by Bacteroidetes (40), and the core xylan utilization cluster identified in this study provides further support for this prediction.

The majority of the genes that were induced by *P. bryantii* B₁₄ during growth on WAX compared with XA code for proteins that are currently designated hypothetical proteins. This observation underscores the fact that there are large gaps in our current understanding of how polysaccharides are metabolized by *P. bryantii* B₁₄ and other gut-associated bacteria. Whole genome transcriptional profiling represents a useful approach to gain insight into the potential roles of genes with unassigned functions. In this study, a subset of genes with low homology to glycoside hydrolases has been shown to belong to GH family 5 based on biochemical data. These genes were only found within certain members of the Bacteroidetes phylum, which are resident within the alimentary tract of humans or ruminants. Most of these GH5 genes occur near the conserved xylan utilization cluster in the genome (Fig. 7; *P. copri*, ORF6092; *P. buccae*, ORF0844, *Bacteroides* sp. 2_2_4, ORF3750; *B. intestinalis*, ORF4213; *B. cellulosilyticus*, ORF3415; *B. eggerthii*, ORF1299), which suggests that they may be directly involved in the degradation of xylan. BeXyn5A and BiXyn5A contain putative signal peptidase II cleavage sites, raising the possibility that the two proteins are anchored on the outside of the cell and perhaps function coordinately with the core xylan utilization cluster.

All of the GH5 proteins identified in this study possess N- or C-terminal stretches of amino acids that did not align with known domains in either the Pfam or the NCBI conserved

Xylan Degradation in the Bacteroidetes

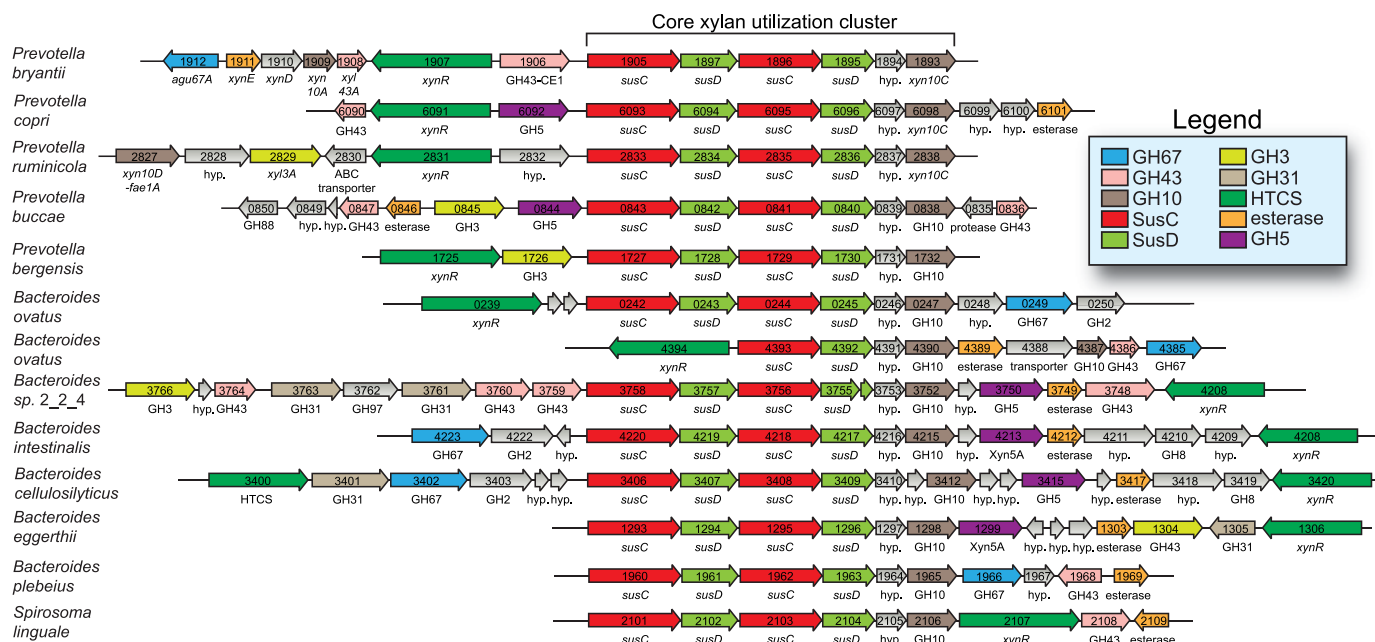


FIGURE 7. Core xylan utilization system is conserved among certain species within the phylum Bacteroidetes. The *P. bryantii* B_{1,4} endoxylanase, Xyn10C, was used as the query sequence in a BLASTp search of the GenBank™ database. The genomic context is shown for each of the top BLASTp hits. Only the region that contains genes with predicted roles associated with xylan deconstruction are shown. Genes are color-coded based on their predicted roles as indicated in the legend. ORF numbers are indicated within each of the genes as derived from the genome project for each organism in the GenBank™ database.

domains database (Table 3). Whether or not these regions represent functional domains is currently unclear. The two *Bacteroides* proteins (BeXyn5A and BiXyn5A) share 78% identity at the amino acid level and also share similar domain organizations with both proteins possessing a C-terminal bacterial Ig2-like domain. The function of this C-terminal extension is currently unknown; however, the Ig2-like domain is predicted to be involved in cell surface adhesion (41). Many xylan-degrading enzymes are associated with carbohydrate-binding modules within a single polypeptide, and it is possible that the Ig2-like domain serves a carbohydrate binding function. Further studies in our laboratory will focus on delineating the functional role of this domain in BeXyn5A and BiXyn5A.

Despite the fact that the three enzymes characterized in this study are clearly related to each other at the amino acid sequence level, they exhibited differences in the products released from WAX. The observation that BeXyn5A (ORF1299, Table 3) synergizes with Ara43A, whereas BiXyn5A (ORF4213, Table 3) and PbXyn5A (ORF0150, Table 3) do not exhibit synergy with Ara43A, clearly indicates that there is a fundamental difference in the enzymatic activities among these enzymes, most likely originating from the GH5 active site domain.

Two additional genes (*P. bryantii* B_{1,4} ORF0336 and *B. intestinalis* ORF1125, Table 3), encoding similar GH5 modules as those found in the enzymes described above, were expressed. Both proteins exhibited endoxylanase activity, and the gene products were named PbXyn5B and BiXyn5B (supplemental Fig. S8). In addition to the GH5 module, BiXyn5B also contains a GH43 domain and is therefore different from BiXyn5A.

Recently, a large number of genome sequences have been made available for human colonic bacteria through the human microbiome project (42). These genome sequences provide a wealth of information on the genome contents of commensal

microbes within the human gut microbiome; however, proper annotation of these genes is critical to interpreting the genomic data in terms of the metabolic repertoire of the microbial community. In this study, transcriptional profiling of a rumen bacterium led to the assignment of function to a group of hypothetical proteins within the rumen *Prevotella* spp. and human colonic *Bacteroides* spp. Furthermore, this study has provided insights that suggest a conserved mechanism for xylan utilization among members of the phylum Bacteroidetes.

Acknowledgments—We thank Shosuke Yoshida, Yejun Han, Michael Iakiviak, and Xiaoyun Su of the Energy Biosciences Institute for valuable scientific discussions and Hiroshi Miyagi for technical assistance. We also thank members of the North American Consortium for Genomics of Fibrolytic Ruminant Bacteria for access to the partial genome sequence of *P. bryantii* B_{1,4}, Alvaro Hernandez and Chris Wright of the W. M. Keck Center for Comparative and Functional Genomics for assistance with Illumina sequencing, and Mark Band from the same center for assistance with microarray analyses.

REFERENCES

- Dodd, D., and Cann, I. O. (2009) *GCB Bioenergy* **1**, 2–17
- Stevenson, D. M., and Weimer, P. J. (2007) *Appl. Microbiol. Biotechnol.* **75**, 165–174
- Edwards, J. E., McEwan, N. J., Travis, A. J., and Wallace, R. J. (2004) *Antonie van Leeuwenhoek* **86**, 263–281
- Dodd, D., Kiyonari, S., Mackie, R. I., and Cann, I. K. (2010) *J. Bacteriol.* **192**, 2335–2345
- Miyazaki, K., Miyamoto, H., Mercer, D. K., Hirase, T., Martin, J. C., Kojima, Y., and Flint, H. J. (2003) *J. Bacteriol.* **185**, 2219–2226
- Miyazaki, K., Martin, J. C., Marinsek-Logar, R., and Flint, H. J. (1997) *Anaerobe* **3**, 373–381
- Gasparic, A., Martin, J., Daniel, A. S., and Flint, H. J. (1995) *Appl. Environ. Microbiol.* **61**, 2958–2964
- Gasparic, A., Marinsek-Logar, R., Martin, J., Wallace, R. J., Nekrep, F. V.,

- and Flint, H. J. (1995) *FEMS Microbiol. Lett.* **125**, 135–141
9. Dodd, D., Kocherginskaya, S. A., Spies, M. A., Beery, K. E., Abbas, C. A., Mackie, R. I., and Cann, I. K. (2009) *J. Bacteriol.* **191**, 3328–3338
 10. Flint, H. J., Whitehead, T. R., Martin, J. C., and Gasparic, A. (1997) *Biochim. Biophys. Acta* **1337**, 161–165
 11. Morrison, M., Daugherty, S. C., Nelson, W. C., Davidsen, T., and Nelson, K. E. (2010) *Microb. Ecol.* **59**, 212–213
 12. Miyazaki, K., Hirase, T., Kojima, Y., and Flint, H. J. (2005) *Microbiology* **151**, 4121–4125
 13. Bryant, M. P., Small, N., Bouma, C., and Chu, H. (1958) *J. Bacteriol.* **76**, 15–23
 14. Aziz, R. K., Bartels, D., Best, A. A., DeJongh, M., Disz, T., Edwards, R. A., Formsma, K., Gerdes, S., Glass, E. M., Kubal, M., Meyer, F., Olsen, G. J., Olson, R., Osterman, A. L., Overbeek, R. A., McNeil, L. K., Paarmann, D., Pazzian, T., Parrello, B., Pusch, G. D., Reich, C., Stevens, R., Vassieva, O., Vonstein, V., Wilke, A., and Zagnitko, O. (2008) *BMC Genomics* **9**, 75
 15. Baggerly, K. A., Deng, L., Morris, J. S., and Aldaz, C. M. (2003) *Bioinformatics* **19**, 1477–1483
 16. Kent, W. J. (2002) *Genome Res.* **12**, 656–664
 17. Bakir, M. A., Kitahara, M., Sakamoto, M., Matsumoto, M., and Benno, Y. (2006) *Int. J. Syst. Evol. Microbiol.* **56**, 151–154
 18. Emanuelsson, O., Brunak, S., von Heijne, G., and Nielsen, H. (2007) *Nat. Protoc.* **2**, 953–971
 19. Gill, S. C., and von Hippel, P. H. (1989) *Anal. Biochem.* **182**, 319–326
 20. Teather, R. M., and Wood, P. J. (1982) *Appl. Environ. Microbiol.* **43**, 777–780
 21. Lever, M. (1972) *Anal. Biochem.* **47**, 273–279
 22. Wang, Z., Gerstein, M., and Snyder, M. (2009) *Nat. Rev. Genet.* **10**, 57–63
 23. Ozaki, K., Shikata, S., Kawai, S., Ito, S., and Okamoto, K. (1990) *J. Gen. Microbiol.* **136**, 1327–1334
 24. Altschul, S. F., Madden, T. L., Schäffer, A. A., Zhang, J., Zhang, Z., Miller, W., and Lipman, D. J. (1997) *Nucleic Acids Res.* **25**, 3389–3402
 25. Shirai, T., Ishida, H., Noda, J., Yamane, T., Ozaki, K., Hakamada, Y., and Ito, S. (2001) *J. Mol. Biol.* **310**, 1079–1087
 26. Hespell, R. B., Wolf, R., and Bothast, R. J. (1987) *Appl. Environ. Microbiol.* **53**, 2849–2853
 27. Dehority, B. A. (1967) *Appl. Microbiol.* **15**, 987–993
 28. Dehority, B. A. (1966) *J. Bacteriol.* **91**, 1724–1729
 29. Salyers, A. A., Balascio, J. R., and Palmer, J. K. (1982) *J. Food Biochem.* **6**, 39–56
 30. Chassard, C., Goumy, V., Leclerc, M., Del'homme, C., and Bernalier-Donadille, A. (2007) *FEMS Microbiol. Ecol.* **61**, 121–131
 31. Salyers, A. A., Gherardini, F., and O'Brien, M. (1981) *Appl. Environ. Microbiol.* **41**, 1065–1068
 32. Chassard, C., and Bernalier-Donadille, A. (2006) *FEMS Microbiol. Lett.* **254**, 116–122
 33. Chassard, C., Delmas, E., Lawson, P. A., and Bernalier-Donadille, A. (2008) *Int. J. Syst. Evol. Microbiol.* **58**, 1008–1013
 34. Mirande, C., Kadlecikova, E., Matulova, M., Capek, P., Bernalier-Donadille, A., Forano, E., and Bera-Maillet, C. (2010) *J. Appl. Microbiol.* **109**, 451–460
 35. Weaver, J., Whitehead, T. R., Cotta, M. A., Valentine, P. C., and Salyers, A. A. (1992) *Appl. Environ. Microbiol.* **58**, 2764–2770
 36. Sonnenburg, E. D., Sonnenburg, J. L., Manchester, J. K., Hansen, E. E., Chiang, H. C., and Gordon, J. I. (2006) *Proc. Natl. Acad. Sci. U.S.A.* **103**, 8834–8839
 37. Shipman, J. A., Berleman, J. E., and Salyers, A. A. (2000) *J. Bacteriol.* **182**, 5365–5372
 38. Koropatkin, N. M., Martens, E. C., Gordon, J. I., and Smith, T. J. (2008) *Structure* **16**, 1105–1115
 39. D'Elia, J. N., and Salyers, A. A. (1996) *J. Bacteriol.* **178**, 7180–7186
 40. Martens, E. C., Koropatkin, N. M., Smith, T. J., and Gordon, J. I. (2009) *J. Biol. Chem.* **284**, 24673–24677
 41. Kelly, G., Prasannan, S., Daniell, S., Fleming, K., Frankel, G., Dougan, G., Connerton, I., and Matthews, S. (1999) *Nat. Struct. Biol.* **6**, 313–318
 42. Turnbaugh, P. J., Ley, R. E., Hamady, M., Fraser-Liggett, C. M., Knight, R., and Gordon, J. I. (2007) *Nature* **449**, 804–810
 43. Cantarel, B. L., Coutinho, P. M., Rancurel, C., Bernard, T., Lombard, V., and Henrissat, B. (2009) *Nucleic Acids Res.* **37**, D233–D238